Collapse of directed functional hierarchy under classical serotonergic psychedelics

Jakub Vohryzek[1,2], Morten L. Kringelbach[2,3,4], Edmundo Lopez-Sola[1,5], Elvira Garcia-Guzmán[1], Christopher Timmermann[6], Leor Roseman[6], Enzo Tagliazucchi[7,8], Giulio Ruffini[5], Robin Carhart-Harris[9,10], Gustavo Deco[1,10], Yonatan Sanz Perl[1,10]

1. Center for Brain and Cognition, Computational Neuroscience Group, Department of Information and Communication Technologies, Universitat Pompeu Fabra, Barcelona, Spain
2. Centre for Eudaimonia and Human Flourishing, Linacre College, University of Oxford, UK
3. Department of Psychiatry, University of Oxford, Oxford, United Kingdom
4. Centre for Music in the Brain, Aarhus University, Aarhus, Denmark
5. Brain Modeling Department, Neuroelectrics, 08035 Barcelona, Spain
6. Center for Psychedelic Research, Department of Brain Sciences, Imperial College London, London SW7 2AZ, UK
7. Universidad de Buenos Aires, Facultad de Ciencias Exactas y Naturales, Departamento de Física, and CONICET - Universidad de Buenos Aires, Instituto de Física Aplicada e Interdisciplinaria (INFINA). Buenos Aires, Argentina
8. Latin American Brain Health Institute (BrainLat), Universidad Adolfo Ibañez, Santiago, Chile
9. Departments of Neurology and Psychiatry, University of California San Francisco, San Francisco 94143, USA
10. Institució Catalana de la Recerca i Estudis Avançats (ICREA), Barcelona, Spain

Abstract

It has been proposed that psychedelics induce profound functional changes to the hierarchical organisation of the human brain. Yet the term hierarchy is currently not well-defined in neuroscience. Here, we use a precise definition of hierarchy, grounded in the theory of thermodynamics, which allows the quantification of temporal asymmetry in the directionality of information flow. We quantified the changes to the directed functional hierarchy of the brain under three classical serotonergic psychedelics – psilocybin, LSD and DMT. We found that all three psychedelics induce a reduction of the directed functional hierarchy, such that they display lower levels of global and network temporal asymmetry and a contraction of the two main patterns of variation of temporal asymmetry. Crucially, our results imply that the brain's directed functional hierarchy is collapsed under psychedelics, interpreted as yielding a more flexible brain. This enhanced flexibility in brain organisation under psychedelics may underpin the altered cognition and behaviour observed during these states, and, possibly afterwards, be suggestive of therapeutic potential.

Introduction

Psychedelic intervention has garnered substantial attention in recent years for its ability to induce profound functional reorganisation within the human brain, both in the acute and long-term phases of its effects[1]. Understanding these changes is important not only for a comprehensive grasp of the underlying neurobiology but also for discovering the mechanisms underlying potential therapeutic

applications[2-4]. The traditional approach addressing this question has focused on the functional interactions between brain regions and has investigated whether the psychedelic experience induces changes in the functional hierarchy [5-9]. Here, we tackle this question by investigating the brain's hierarchical organisation under psychedelics using thermodynamics principles to quantify the temporal asymmetry in information flow, and thus defining brain's temporal hierarchical organisation.

The main hypothesis is that psychedelic interventions desynchronise the brain[1] and change the organisation of the brain by shifting the functional hierarchy, where unimodal regions, related to sensory cortices, become less constrained from the transmodal higher-level cognitive cortices, leading to novel perceptual experiences[10]. In that direction, recent evidence has shown that the principal gradient representing such functional organisation is compressed under psilocybin, LSD and DMT[5,9]. Furthermore, directed functional hierarchy, derived from harmonic decomposition of functional interactions, has been shown to collapse under DMT-induced brain state[8]. Nevertheless, the term 'hierarchy' is currently not well defined in neuroscience and several definitions coexist in the literature[11]. Here we used a concrete definition of hierarchy of a system, namely directed functional hierarchy, that quantifies the temporal asymmetry in the directionality of information flow[12]. Importantly, this definition is theoretically grounded in thermodynamics which defines 'breaking the detailed balance' as a direct measure of asymmetry for any physical system and determines the level of non-equilibrium[12-15].

Recent work has directly quantified temporal hierarchical organisation from spatiotemporal whole-brain data by measuring hierarchy through the level of irreversibility of brain signal. Indeed, such definition of hierarchy has revealed differential ways of how psilocybin and escitalopram (an antidepressant drug) work in rebalancing brain dynamics in depression[16], as well as, has implicated the importance of reorganisation of fronto-striatal-thalamic circuitry in long-term effects of psilocybin[17]. Furthermore, higher levels of asymmetrical information flow have been observed during cognitive tasks implying a hierarchical organisation needed for the specific computations[13,18,19]. Conversely, a lower level of irreversibility has been observed in disorder of consciousness human patients and anesthetized non-human primates suggesting constrained computational capabilities[13,20].

The main idea here is to capture the asymmetry in the temporal processes by comparing time-shifted correlation matrices of neuroimaging data and to examine how this reflects changes to the directed functional hierarchy in the brain under psychedelics. To this end, we leverage previously published dataset of resting-state functional magnetic imaging (fMRI) data from healthy human participants under the effects of three classical serotonergic psychedelics, namely psilocybin[21] (N=9), LSD[22] (N=15) and DMT[9] (N=17), in the acute post-intervention stage. Crucially, we compute the global and network levels of temporal asymmetry characterizing which aspects of the brain's

distributed functional organisation are consistently involved in psychedelic effects despite the different drugs. We also investigate how the temporal asymmetry hierarchical reconfiguration changes across different spatial scales by changing the graining of the parcellation ranging from 100 to 1000 brain regions in the Schaefer parcellations[23]. Finally, we compute the functional gradients on the temporal asymmetry matrices to directly quantify the functional organisation of directed functional hierarchy in terms of uni-and transmodal modes.

Overall, the results suggest that acute effects of psychedelics induce a flattening of the hierarchical functional organisation, showing lower levels of global and networks temporal asymmetry than resting-state controls participants. Importantly, considering that one defining feature of non-equilibrium behaviour in living organisms is their dependence on the spatial scale[24], i.e., few available macroscopic observables may be the result of averaging over non-equilibrium degrees of freedom, we investigate whether the temporal asymmetry in brain dynamics is intrinsically related with the spatial scale in which the brain signals are considered. We found that coarse-grained parcellations are not optimal for describing the psychedelic effects in terms of temporal asymmetry hierarchy reconfiguration, while parcellations from 300 regions and above seems to capture the reconfiguration. The time functional gradients analysis also shows a collapse of the first two components during psychedelic effects mainly in visual and somatomotor areas aligned with previous findings[5,9]. As such, the results demonstrate that temporal asymmetry encodes relevant features of whole-brain functional organisation during acute psychedelics effects, providing evidence that hierarchy is flattened making brain organisation more accessible and adaptable in support of increased flexibility.

Results

Overview

In order to fully appreciate the functional changes under psychedelics, new advanced methods are needed. Our goal here is to propose a more principled measure of directed functional hierarchy inspired by tools from the theory of thermodynamics. We defined directed functional hierarchy as the amount of asymmetry in the brain. To do so, we quantified temporal asymmetry, in terms of time-shifted correlations, to capture the breaking of the detailed balance. Then, we computed the magnitude of temporal asymmetry for three different psychedelic-induced brain states – DMT, LSD and Psilocybin (**Figure 1A**). We measured the global decrease of the magnitude of temporal asymmetry by computing the Fano factor over the distribution of pairwise values of the magnitude of temporal asymmetry between various regions (**Figure 1B**). Then, we applied the same measure of temporal asymmetry in terms of resting-state networks calculating within and between network magnitude of temporal asymmetry (**Figure 1C**). Finally, we explored the functional organisation of temporal asymmetry for the two principal gradients of the magnitude of temporal asymmetry matrix (**Figure 1D**).

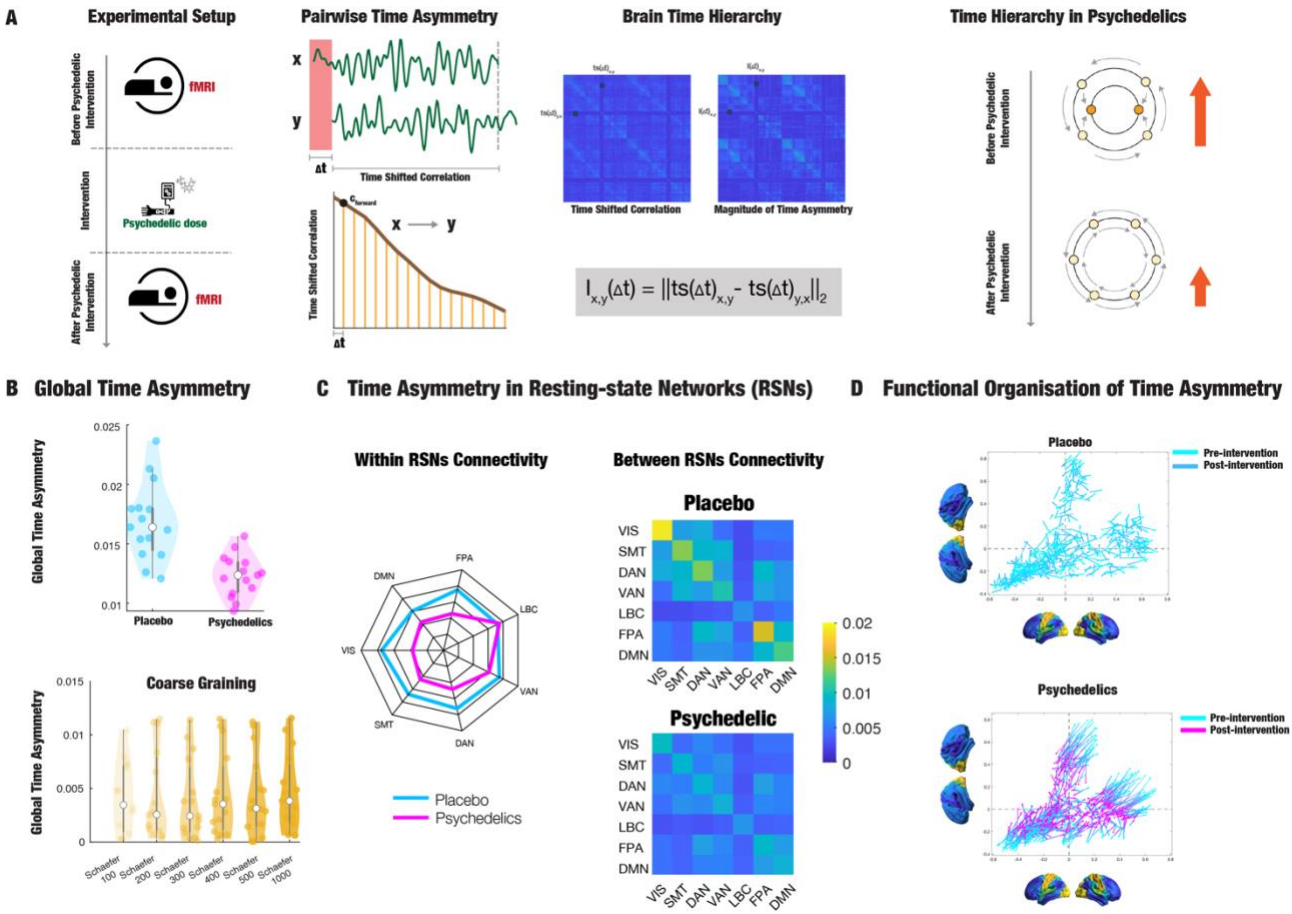

Figure 1. Calculation of Brain Directed functional hierarchy in Psychedelic State. A) *Neuroimaging fMRI data of whole-brain dynamics before and during the intervention with psychedelic compounds – psilocybin (n=9), LSD (n=15)*

and DMT (n=17) (see Methods). The pairwise temporal asymmetry is measured as a time-shifted correlation between brain regions of interest x and y with a time shift of 1 TR. At the whole-brain level the temporal asymmetry is summarized in an asymmetric matrix represented by the Time Shifted Correlation matrix. The Magnitude of temporal asymmetry is defined as the square of the difference between time-shifted correlations of regions x and y, and time-shifted correlations of regions y and x. The working hypothesis is that directed functional hierarchy in the psychedelic-induced state decreases compared to the pre-intervention state. ***B)*** *Global temporal asymmetry, calculated as the Fano Factor of the distribution of regional magnitudes of temporal asymmetry. The influence of coarse graining on the Global temporal asymmetry was performed for different spatial scales defined by the multiscale Schaefer parcellation – 100, 200, 300, 400, 500 and 1000 brain regions.* ***C)*** *temporal asymmetry in resting-state networks (RSNs), calculated as the Fano Factor of the distribution of regional magnitudes of temporal asymmetry within and between given resting-state networks.* ***D)*** *Functional organisation of temporal asymmetry was derived for the two principal components of the magnitude of temporal asymmetry matrix explaining equal variance of the data for the three psychedelic datasets.*

Global temporal hierarchical brain organisation is flattened during psychedelics states

We investigated how the directed functional hierarchy is reorganised during psychedelics state based on thermodynamics definition to capture the directionality of temporal information flow. We computed the temporal asymmetry from the fMRI time series extracted from different psychedelic drugs and the corresponding placebo condition (**Figure 2)**. In brief, our measures of temporal asymmetry are based on the shifted functional connectivity matrix, computed as the pairwise Pearson's correlation of the time series with a temporal shift between pairs of signals. In that way, we obtained an asymmetrical matrix that contains how the signal *j* in time $t + \Delta t$ is affected by the signal *i* in time *t* in the entry *ij*, and the vice versa in the entry *ji* (see Methods). We then define the temporal asymmetry matrix as the absolute value of the difference between the shifted correlation matrix and its transpose (a symmetric square matrix). We quantified the global level of the magnitude of temporal asymmetry by computing the Fano factor, i.e., the ratio between the mean and the standard deviation across all entries of these matrices, for each participant in each condition and dataset. We found that the global magnitude of temporal asymmetry significantly decreases under the effects caused by different psychedelic drugs (DMT (DMT post vs. DMT pre, $p<1x10^{-4}$, DMT post vs. PCB post, $p<1x10^{-4}$, PCB post vs. PCB pre, p=0.419), LSD (LSD post vs. LSD pre, $p=3x10^{-4}$) and psilocybin (PSILO post vs. PSILO pre, p=0.022, PSILO post vs. PCB post, p=0.057, PCB post vs. PCB pre, p=0.79)) compared with the temporal asymmetry before dose administration or with placebo effects (**Figure 2A**). These results were obtained using a fine-grained parcellation consisted of 1000 cortical brain regions[23]. Based on these changes, we can interpret that the directed functional hierarchy is flattened during the psychedelic state.

Considering that the temporal asymmetry of a system is dependent on the spatial scale, we also investigated the effect of the spatial graining by means of different size cortical parcellation on the hierarchical reorganisation during psychedelic state. To do so, we exhaustively computed the

temporal asymmetry for six different brain parcellations ranging from 100 to 1000 regions as defined by Schaefer and colleagues[23]. In **Figure 2B** we show how the difference between the temporal asymmetry before and after psychedelic states increases with finer parcellations, while the statistical comparison becomes more significant, as measured by the reduction of the p-value of a paired t-test. Importantly, we noticed that for the three drugs differences between pre and post dose administration are significant in all the cases for parcellation resolutions of more than 300 brain regions. For the DMT and LSD drugs the results are significant across all parcellation resolutions.

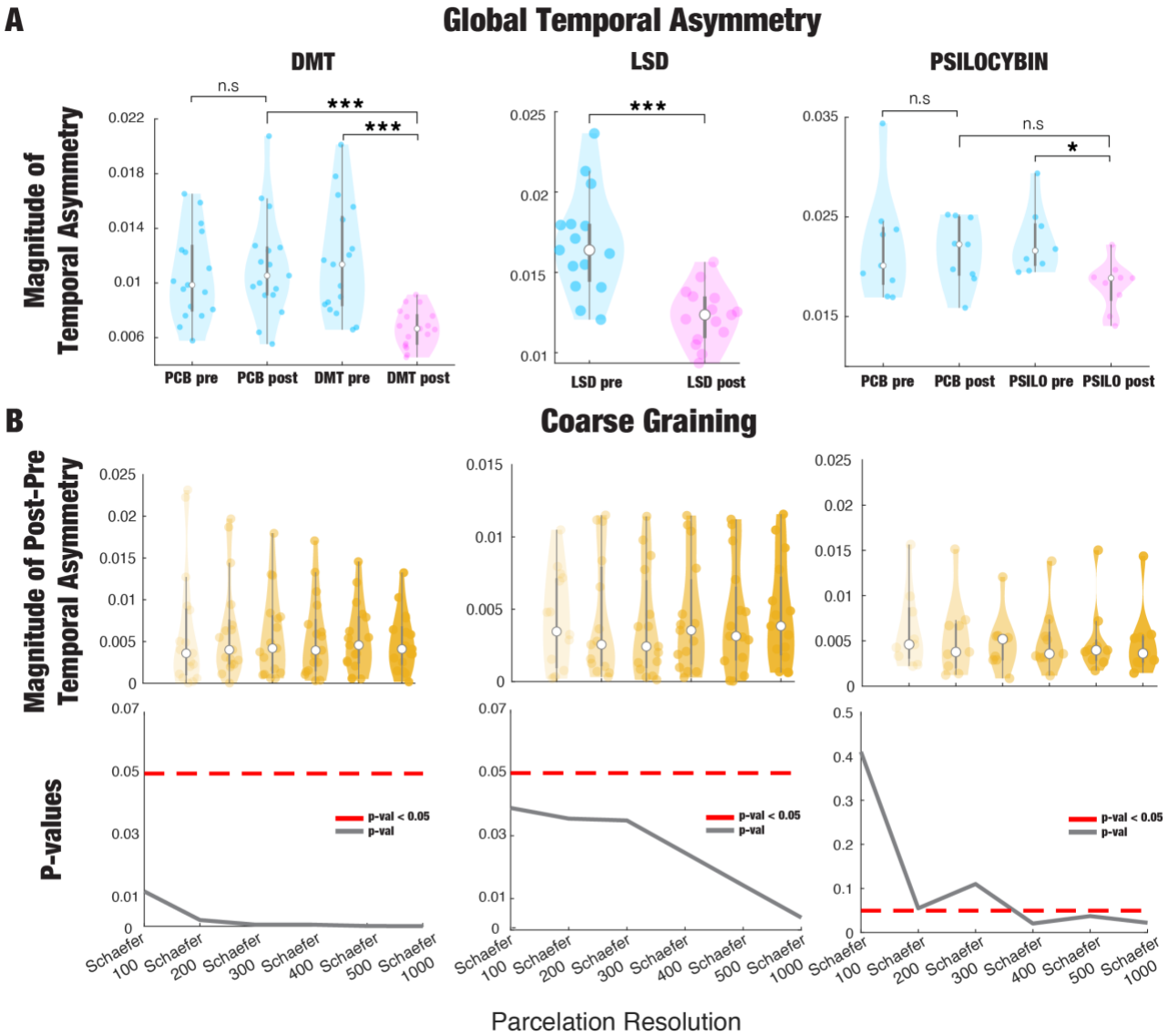

Figure 2. Global reconfiguration of directed functional hierarchy during psychedelic effects. A) *We computed the magnitude of temporal asymmetry for each condition in the three psychedelic datasets for Schaefer 1000 parcellation. We found that post psychedelic administration condition (pink violin plots) the temporal asymmetry is significantly lower compared with the placebo condition (PCB) pre and post injection, and compared with the before drug administration (blue violin plots) (two-tailed paired t-test, DMT dataset: DMT post vs. DMT pre, $p<10^{-4}$, DMT post vs. PCB post, $p<10^{-4}$, PCB post vs. PCB pre, $p=0.419$., LSD dataset: LSD post vs. LSD pre, $p=3x10^{-4}$, PSILOCYBIN dataset: PSILO post vs. PSILO pre, $p=0.022$, PSILO post vs. PCB post, $p=0.057$, PCB post vs. PCB pre, $p=0.79$, * $p<0.05$, *** $p<0.001$).* ***B)*** *We found that the differences between before and after doses administration increases with the resolution of the parcellation while becomes more significant in terms of the reduction of the p-value (two-tailed paired t-test).*

Functional system temporal asymmetry is reconfigured during psychedelics states

Following our results at the global level, we focused here on the changes that temporal asymmetry undergoes at the functional system level, as it is believed to reflect the role that different networks play in temporal hierarchical reconfiguration. We computed the temporal asymmetry for each of the functional resting state networks (RSN), namely the Yeo 7 RSN[25], for each participant with each psychedelic drug and for the placebo condition (PCB) before and after administration. The within RSN temporal asymmetry was computed by averaging weights within a network, and between RSN temporal asymmetry was computed by averaging weights between two networks. First, we investigated how the temporal asymmetry is modified within each RSN across conditions (**Figure 3A**). We found that the default mode network (DMN), frontoparietal network (FPA), and dorsal attention network (DAN) significantly, and consistently for the three psychedelics, reduce the magnitude of temporal asymmetry (DMT: DMT post vs. DMT pre; VIS - $p<10^{-4}$, SMT - $p<10^{-4}$, DAN – p=0.014. VAN - p=0.035. LBC p=0.809, FPA - $p<10^{-4}$, DMN - p=0.0052, PCB post vs. PCB pre; n.s., LSD: LSD post vs. LSD pre; VIS - $p<10^{-4}$, SMT – p=0.054, DAN - p=0.014. VAN - p=0.015. LBC p=0.184, FPA – p=0.036, DMN – p=0.002, PSILO: PSILO post vs. PSILO pre; VIS – p=0.335, SMT – p=0.474, DAN – p=0.012. VAN – p=0.851. LBC p=0.448, FPA – p=0.015, DMN – p=0.006, PCB post vs. PCB pre; n.s). Secondly, we assessed the reconfiguration of temporal asymmetrical interactions between RSNs during the psychedelic state induced by different drugs. In **Figure 3B**, we display the interaction matrices before and after dose administration (DMT and psilocybin) and after dose administration and placebo condition (DMT, LSD, and psilocybin). We found that interactions involving the DMN and FPA networks are significantly altered during the psychedelic state compared with the PCB condition and before dose administration (Table S1). Importantly, for the DMT and psilocybin dataset, in which we have the control PCB experiment, we noticed almost no significant differences when comparing before and after PCB administration, supporting the hypothesis that psychedelic drugs are responsible for reshaping temporal asymmetry interactions.

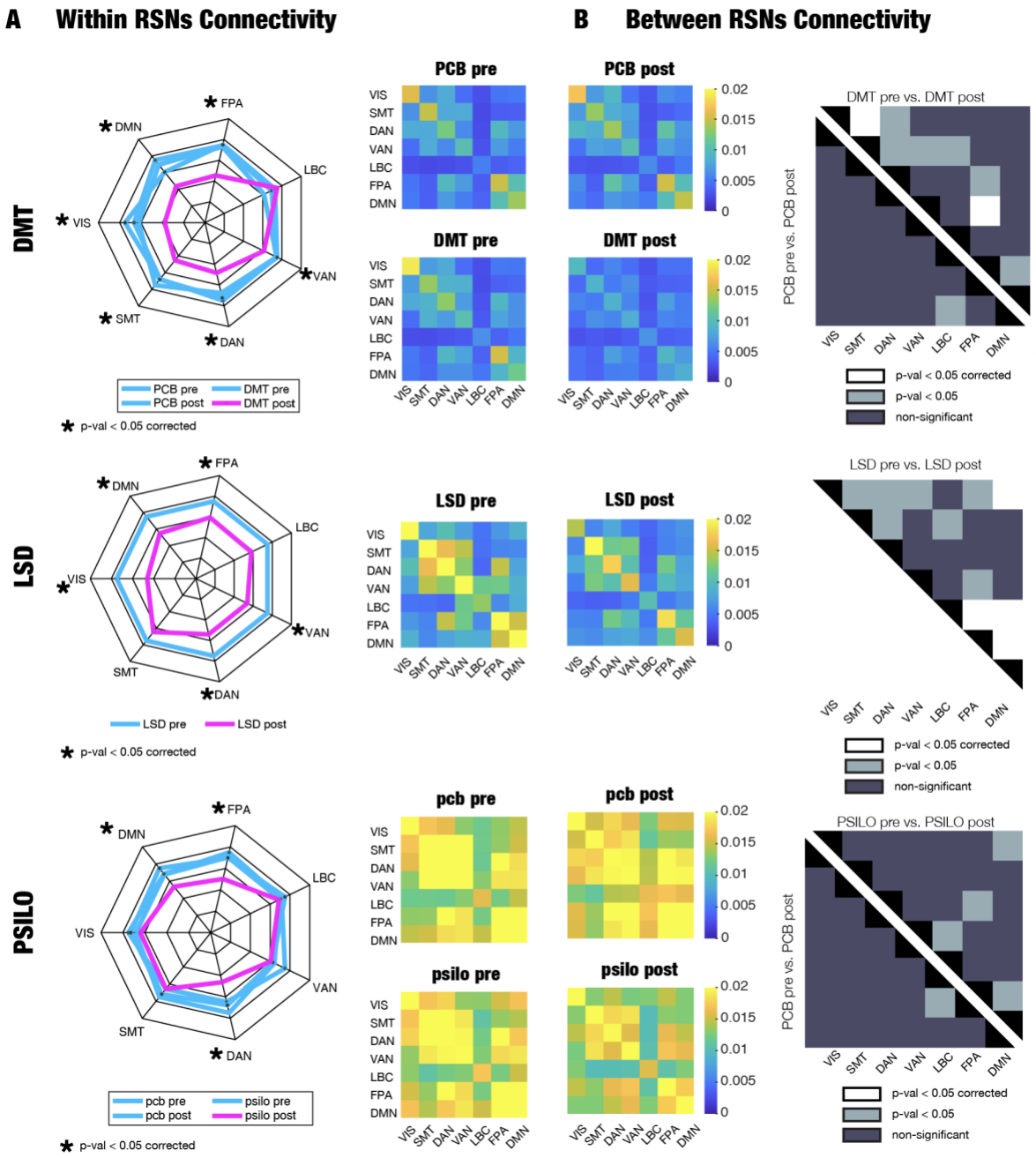

Figure 3. Functional system temporal asymmetry is reconfigured during psychedelics states. *We computed the magnitude of temporal asymmetry for each functional system, namely the Yeo 7 resting state networks, and for each condition in the three datasets.* ***A)*** *We investigated how the magnitude of temporal asymmetry of each RSN is altered during psychedelic state compared with the PCB condition and before the doses administration. We found that DMN, FPA and DAN significantly decrease the magnitude of temporal asymmetry during psychedelic states (two-tailed paired t-test, DMT: DMT post vs. DMT pre; VIS - $p<10^{-4}$, SMT - $p<10^{-4}$, DAN – p=0.014. VAN - p=0.035. LBC p=0.809, FPA - $p<10^{-4}$, DMN - p=0.0052, PCB post vs. PCB pre; n.s., LSD: LSD post vs. LSD pre; VIS - $p<10^{-4}$, SMT – p=0.054, DAN - p=0.014. VAN - p=0.015. LBC p=0.184, FPA – p=0.036, DMN – p=0.002, PSILO: PSILO post vs. PSILO pre; VIS – p=0.335, SMT – p=0.474, DAN – p=0.012. VAN – p=0.851. LBC p=0.448, FPA – p=0.015, DMN – p=0.006, PCB post vs. PCB pre; n.s.. In the figure we report fdr corrected p-values (* p<0.05 corrected).* ***B)*** *We show how the magnitude of temporal asymmetrical interactions between RSN are modified during the psychedelic state. We show the interaction matrices for each dataset and for each condition averaged across participants (first column) and then we assessed the statistical differences between conditions in term of paired t-test false discovery rate corrected (white entries) and without*

correction (grey entries) (rightmost column) (see Table S1). (DMN: default mode; FPA: frontoparietal; LBC: limbic; VAN: ventral attentional; DAN: dorsal attentional; SMT: somatomotor; VIS: visual networks).

Functional gradients organisation of temporal asymmetry is reshaped during psychedelics

A second complementary perspective pertains to the brain's functional gradients organisation on how the temporal hierarchy is altered during the effects of psychedelics. Typically, functional gradients are constructed using principal component analysis or similar nonlinear methods (Diffusion Map Embeddings, Laplacian Eigenmodes, among others [26]) to extract the gradients from functional data. These methods provide a low-dimensional representation of the data by computing the most significant patterns of variation of functional connectivity (FC) in the form of gradients. Specifically, the first functional gradient captures the greatest variation in the functional connectivity organisation[27]. In previous studies, functional gradients were examined during the acute phase following psychedelic administration, revealing a collapse of the first gradient during DMT state measured as the difference between the minimum and maximum range of the functional data projected in that first gradient[9]. Here, we hypothesize that the functional organisation of the temporal asymmetry will also be reshaped during the effects of psychedelics, showing differences in the range of the projections of the temporal asymmetry on the gradients. While, traditionally, the number of gradients is selected by choice, often focusing on the first gradient because of its primary importance in terms of explaining most of the variance in the data, here we chose the number of gradients that have given us the same variance explained across each dataset.

Therefore, for each dataset, we obtained the first two gradients of temporal asymmetry, as we found that this is the minimum number of gradients showing not significant differences in the explained variance (**Figure S1 and S2**). Consequently, for the rest of the gradient analysis, we considered the first two gradients to assess how functional organisation of the temporal asymmetry is reshaped under psychedelics. **Figure 4A** shows the spatial distribution of the first two temporal asymmetry gradients for the three different psychedelics drugs in Schaefer 400 parcellations using PCA methods implemented in the BrainSpace Toolbox[26]. We also show the associations of gradients loading to each RSN for each condition in each dataset for the first two gradients. We noticed that, consistently for the three datasets, the first gradient separates the somatomotor network with default mode and frontoparietal networks, and the second gradient separates the visual with higher-order networks. At individual level, we investigated the gradient contraction in the two-dimensional space determined by the first two gradients. We projected the loading of each brain region in this two-dimensional space for each drug pre and post administration (DMT, LSD and PSILOCYBIN) and pre and post PCB doses (DMT and PSILOCYBIN) and we quantified the gradient contraction by computing the surface that loading projections are spanning in each case. We found that these gradient

surfaces are lower during psychedelic state (two-tailed paired t-test, DMT dataset: DMT post vs. DMT pre, $p=3x10^{-4}$, DMT post vs. PCB post, $p=5x10^{-4}$, PCB post vs. PCB pre, p=0.594, LSD dataset: LSD post vs. LSD pre, p=0.007, PSILOCYBIN dataset: PSILO post vs. PSILO pre, p=0.026, PSILO post vs. PCB post, p=0.883, PCB post vs. PCB pre, p=0.357), showing that psychedelics induce a two-dimensional gradient contraction of the temporal asymmetry functional organisation (**Figure 4B)**.

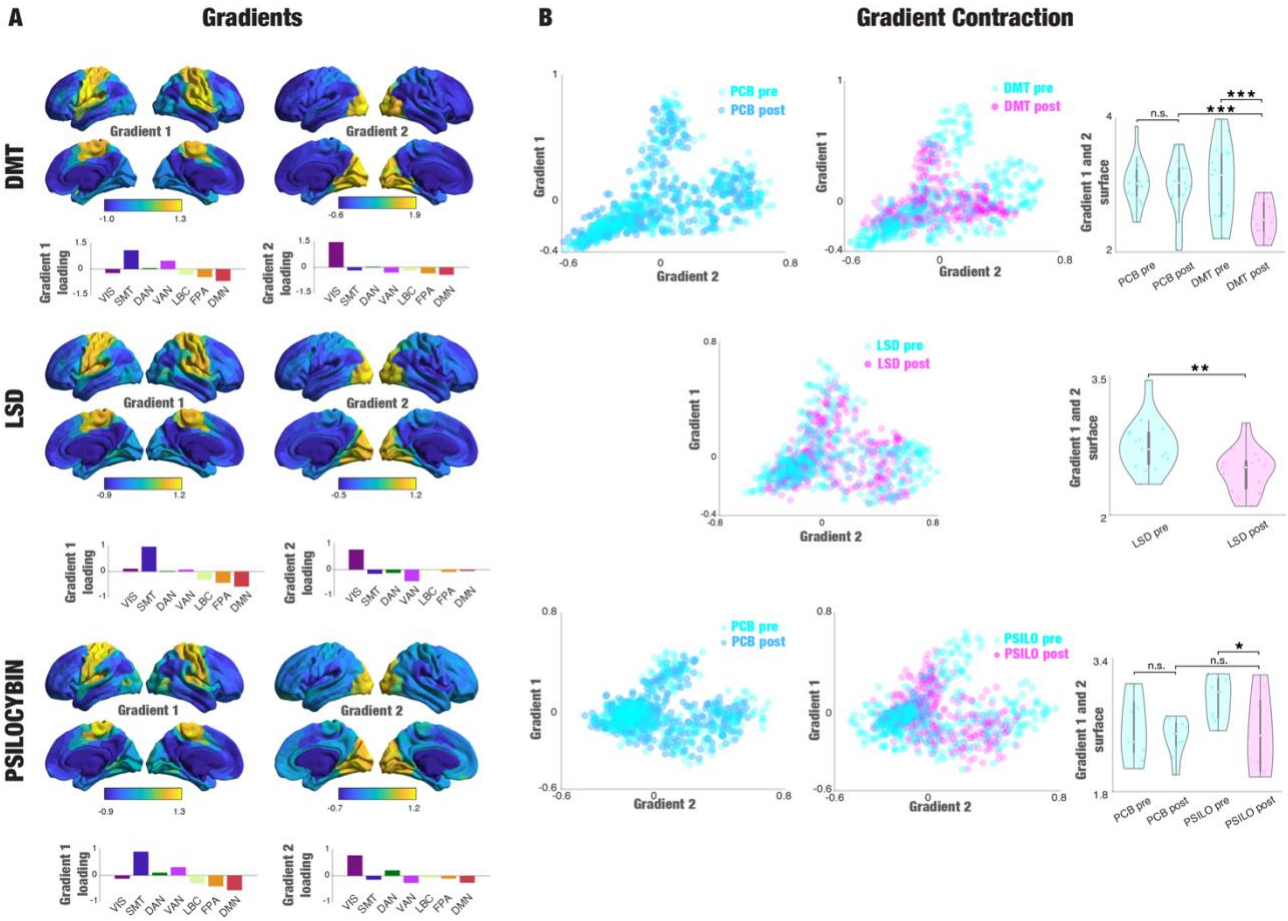

Figure 4. Functional gradients organisation of temporal asymmetry is reconfigured under psychedelic state. A) *We obtain the first two functional gradients of the magnitude of temporal asymmetry for the three datasets before and after the doses administration (DMT, LSD and PSILOCYBIN), and before and after the PCB intervention (DMT and PSILOCYBIN). The timeseries for this analysis were extracted in Schaefer 400 parcellation, which is the minimum resolution showing significantly results in reshaping the temporal hierarchy during psychedelics (see Figure 2). In the three cases the spatial distribution of both gradients is similar for the three drugs. We found that the amount of variance explained is not significantly different for the three datasets pre and post drug, and PCB administration when the first two gradients are considered (see Figure S1). We related the gradients loading, i.e., the projection of each brain region into the gradients, with each RSN for each condition in each dataset for the first two gradients. Consistently for the three datasets, the first gradient separates the somatomotor network with default mode and frontoparietal networks, and the second gradient separates the visual with higher-order networks.* ***B)*** *We quantified the reshaping of the functional organisation of the temporal asymmetry by computing the surface spanned by the projections of the loadings in the two-dimensional space generated by the first two gradients. We found a gradient surface contraction during psychedelic states (two-tailed paired t-test, DMT dataset: DMT post vs. DMT pre, $p=3x10^{-4}$, DMT post vs. PCB post, $p=5x10^{-4}$, PCB post*

*vs. PCB pre, p=0.594, LSD dataset: LSD post vs. LSD pre, p=0.007, PSILOCYBIN dataset: PSILO post vs. PSILO pre, p=0.026, PSILO post vs. PCB post, p=0.883, PCB post vs. PCB pre, p=0.357, * p<0.05, ** p<0.01, *** p<0.001).*

Regional level reshaping of functional organisation of directed functional hierarchy under psychedelics

Since psychedelic drugs induce a surface contraction in the two-dimensional space defined by the first two functional gradients of temporal asymmetry, we asked whether this contraction could be evaluated at the regional level in that space. To do so, we projected the loadings of each region in the space given by the first two functional gradients of temporal asymmetry pre/post drug administrations (DMT, LSD and PSILOCYBIN) and pre/post-PCB administration (DMT and PSILOCYBIN). In **Figure 5A**, we show the projections of the 400 brain regions for each case, labelled with different colours corresponding to regions in Yeo7 RSNs.We then tracked each region in that space during the reshaping of the gradients between pre/post drug and pre/post-PCB administration (**Figure 5B**). We identified each region with a trajectory in two-dimensional space moving from cyan dots (pre) to magenta dots (post psychedelic) and to blue dots (post placebo), allowing us to quantify this reshaping in terms of distances in that space. We measured the reshaping of the gradients by quantifying the distance of the trajectory of each region in the pre and post conditions for the DMT and PSILO datasets (**Figure 5C**). We found that the distances are significantly higher for both DMT and PSILO datasets (DMT: p=0.028, PSILO: p=0.019). It is to be noted that for LSD we could not compute this due to the missing placebo condition. Finally, we rendered into brain surfaces the distance that each brain region travels between the psychedelic and non-psychedelic state and for the PCB condition (**Figure 5D)**. Crucially, somatomotor and visual areas seem to be involved in the reshaping of the gradients at the regional level as well as regions of the default mode network.

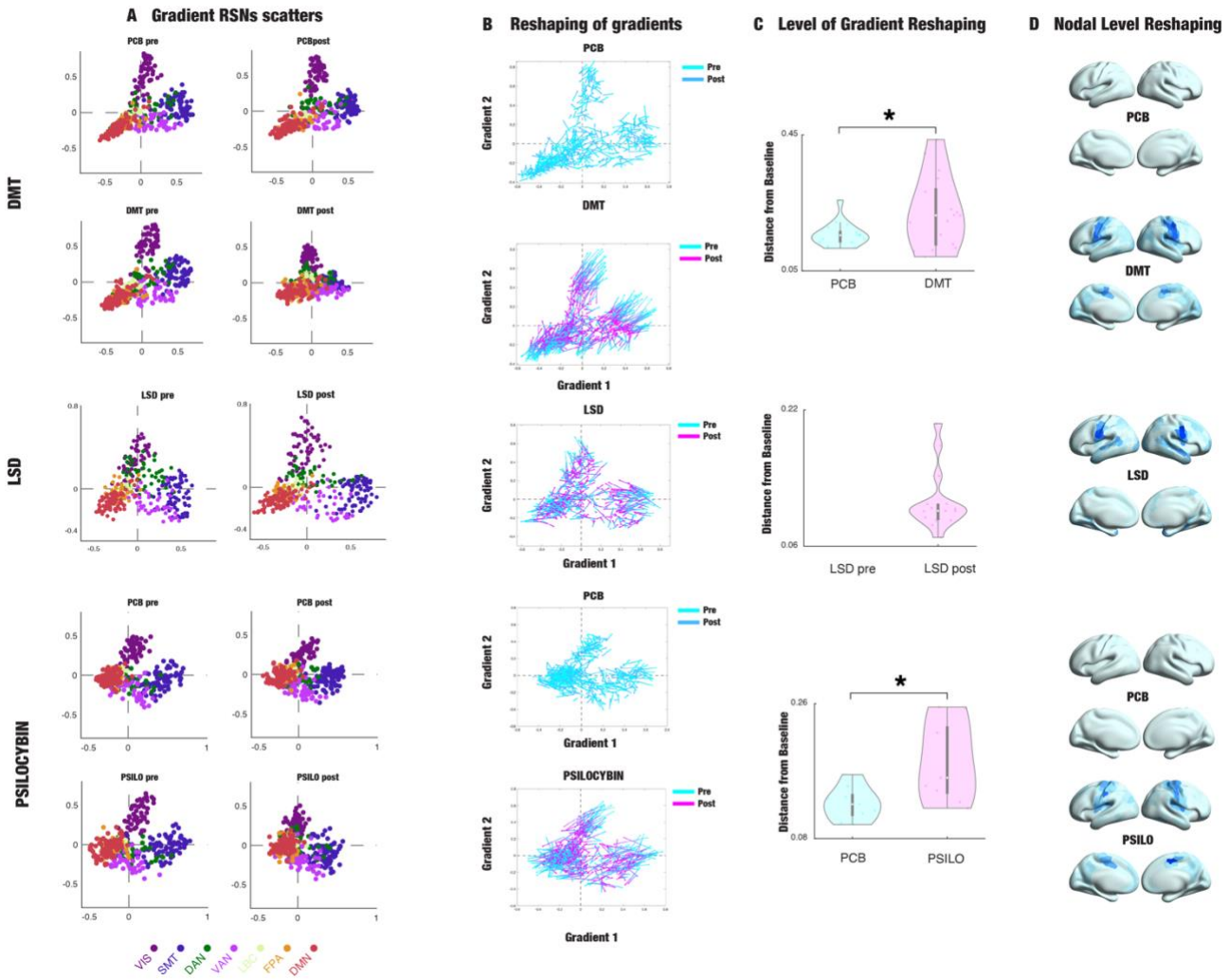

Figure 5. Regional level reshaping of the functional organisation of temporal asymmetry during psychedelic state*. A) We project each brain region (each dot in the plots) on the two firsts functional gradients of the magnitude of temporal asymmetry for the three datasets pre/post doses administration (DMT, LSD and PSILO) and pre/post the PCB intervention (DMT and PSILO). The color code is relating each brain region to the corresponding RSN.* ***B)*** *We are representing the trajectories of each brain region when the functional organisation of the magnitude of temporal asymmetry is reshaped during psychedelics. The origin of trajectories is the cyan dot, representing pre (or control condition) while the state post intervention is represented by magenta dots for psychedelic and by blue dots for placebo interventions.* ***C)*** *We quantified the contraction of the two-dimensional gradient space through measuring the distance of each trajectory. We show compared across participants the distances travelled for each region between pre/post DMT and psilocybin with the corresponding pre/post PCB and we found that for DMT and PSILO groups the distances travelled are higher than PCB groups (DMT: p=0.028, PSILO: p=0.019, * p<0.05). We did not perform this comparison for LSD as it does not have the placebo condition and therefore, we only report the distance for pre/post LSD.* ***D)*** *We render brain surfaces with the distance that each brain region travels averaged across participants between the psychedelic and non-psychedelic state and for the PCB conditions in DMT and PSILO.*

Discussion

Overall, our findings suggest that the acute effects of psychedelics lead to a collapse of the functional organisation of the temporal hierarchy, with lower levels of global and network temporal asymmetry

compared to resting-state controls. We also demonstrate that spatial graining by means of different whole-brain parcellation resolutions impacts the estimation of temporal asymmetry information flow reconfiguration during psychedelic states. The analysis of temporal functional gradients also indicates a collapse of the first two components during psychedelic effects, primarily in visual and somatomotor areas. Crucially, our analysis assesses how each brain region is moving in two-dimensional space determined by the first two functional gradients, showing longer trajectories comparing pre- and post-psychedelics with pre- and post-PCB conditions. These results demonstrate that temporal asymmetry encodes significant features of whole-brain functional organisation during acute psychedelic effects, providing evidence that the directed functional hierarchy is flattened, enabling a more flexible and accessible brain organisation.

Currently, within neuroscience the notion of hierarchy is not well defined[12]. This is partly because current scientific fields and methodologies target different aspects of brain organisation[11]. In this paper we applied a precise definition of hierarchy of a system, namely directed functional hierarchy, that computes the level of temporal asymmetry in the directionality of information flow. This description stems from thermodynamics which posits that the 'breaking of the detailed balance' serves as a direct measure of asymmetry for any physical system. Asymmetry in processing is crucial for computation in recurrent neural networks (RNNs) such as the human brain because it allows for directed information flow, dynamic feedback, and the emergence of complex temporal behaviours. Asymmetrically connected neuronal populations enable the network to maintain and evolve internal states over time, a key requirement for tasks involving memory and sequence prediction, and, more generally, computation[28]. In contrast, symmetric or bidirectional connections often cancel out these dynamic effects, limiting the network's ability to compute complex temporal patterns effectively[29-32]. Such definition of hierarchy based on asymmetry differs from previously used approaches that expressed the flattening of functional hierarchies in terms of compression of the principal cortical gradient as derived from static functional connectivity[5,9]. Intuitively, this can be understood by appreciating that the magnitude of temporal asymmetry matrix encodes the amount of directionality of information flow which is not the case in traditional approaches using static functional connectivity.

In the brain, psychedelic action results in enhanced richness of spatiotemporal dynamics. This has been supported by a broadening of the functional states repertoire and increases in temporal complexity while the functional network of the brain reflects a more integrated state with the suppression of individual resting-state networks[33-35]. This corroborates theoretical and empirical works positing that psychedelics collapse the brain's functional hierarchies, and, in effect "flatten the landscape" of brain dynamics[10,36,37]. By escaping deep local minima under psychedelics, the brain practically fosters flexible and adaptative patterns of thought and behaviour. Here, the lower levels

of global and network temporal asymmetry compared to resting-state control participants align with these findings. This is further supported by the gradients analysis showing the contraction of the first two components during psychedelic effects mainly in visual and somatomotor areas. Importantly, our results are highly consistent across three different psychedelic drugs, namely DMT, LSD and psilocybin.

In the context of thermodynamics of living systems, it is well-known that systems need to operate far from thermodynamic equilibrium to perform most of the important biological functions for living. Langton's seminal work showed that maximal computational capability emerges in dynamical systems poised at the "edge of chaos," a regime between order and randomness where complex, structured patterns and universal computation can arise[38]. This insight established a link between criticality and information processing, suggesting that non-equilibrium conditions are integral to meaningful computation. More recently, England's theoretical advances demonstrated that life-like behavior and adaptive organization can naturally emerge as dissipative structures under sustained energy flow[39,40]. By framing biological systems as inherently far-from-equilibrium entities capable of "computing" probabilistic inferences about their environment, this perspective aligns with the notion that non-equilibrium conditions are not only conducive to complexity but essential for sustaining processes that both generate and utilize information in a functionally meaningful way. Landauer's principle further provides a thermodynamic foundation for this relationship, explicitly linking information processing to energy dissipation and entropy production[41]. This connection extends to Friston's free energy principle[42], which conceptualizes biological systems as nonequilibrium steady-state engines that minimize variational free energy—a statistical and information-theoretic quantity—while continuously dissipating energy to maintain organized, inference-driven states. Together, these lines of inquiry unify thermodynamics, information processing, and adaptive computation under the umbrella of nonequilibrium physics.

At microscopic scales, for instance, enzymatic activity can induce broken detailed balance at the molecular scale driving the system out of equilibrium[43]. At the same time these microscopic mechanisms can drive the system out of equilibrium by breaking the detailed balance at the mesoscopic scales[44]. Nevertheless, the nonequilibrium nature of a system is intrinsically dependent on the spatiotemporal graining, and whether the non-equilibrium dynamics is preserved from a finer to a coarser graining is an open question[45]. The same questions have been posed in brain dynamics, and, while, in general, it is agreed that at the neuronal scale the processes are out-of-equilibrium, it is less clear for macroscopic brain dynamics. Recent studies have investigated, using different methodologies, how whole-brain macroscopic dynamics breaks the detailed balance to hold cognitive functions[15,46] and how the level of non-equilibrium is related with state consciousness[13,14,47] and their alterations during disease[20]. Similarly, recent research has demonstrated that psilocybin and

escitalopram work in different ways for rebalancing brain dynamics in depression, supporting the hypothesis that neuropsychiatric disorders could be closely linked to the breakdown in regions orchestrating brain dynamics from the top of the hierarchy[16]. Here, we investigated the directed functional hierarchy reshaping during psychedelic states based on temporal asymmetry (as a signature of deviation from the equilibrium) and its dependence on the spatial scaling of the system. We addressed this question by exploring different parcellation resolutions. We discovered that coarse-grained parcellations are not optimal for describing the psychedelic effects in terms of temporal asymmetry hierarchy reconfiguration, while parcellations of 300 regions or more seem to capture the reconfiguration effectively.

The breakdown of irreversibility and time-asymmetry under psychedelics can also be interpreted from the point of view of computation and interference with the brain's "modelling engine"[48-50]. Systems performing computations must operate out of equilibrium, as computation inherently involves information processing, state changes, and energy dissipation. Landauer's Principle demonstrates that erasing information incurs a thermodynamic cost, linking computation to entropy generation and irreversibility[41]. Living systems, guided by non-equilibrium thermodynamics, continuously consume energy to maintain ordered structures and perform computations such as gene regulation and neural signaling [51]. Similarly, artificial computational systems, including classical and reversible computers, dissipate energy as they transition between states, further emphasizing that computation is fundamentally a non-equilibrium process[52].

Importantly, our work aims to investigate the temporal asymmetry obtained through the time-shifted correlation, which is often used as a straightforward signature of deviation from equilibrium[53]. Equally, there are different approaches for capturing the breaking of the detailed balance and temporal asymmetry that can be used to investigate the reshaping of the directed functional hierarchy during psychedelics. For instance, Granger Causality or Mutual Information could be considered to quantify the time directionality of the information flow between brain signals[54,55] Also different approaches capturing the non-equilibrium nature of whole-brain dynamics could be considered, such as the generative effective connectivity as proposed by Kringelbach and colleagues[46], or violations from the fluctuation-dissipation theorem proposed by Deco and colleagues[56].

In summary, the present work broadens our understanding of the link between temporal asymmetry in information flow and the organisation of distributed function and the impact of psychedelics on brain dynamics, as well as the interplay between local changes and the architecture of whole-brain directed functional organisation.

Methods

In this section we provide all the details of the empirical neuroimaging data for all the three datasets used in this study.

Participants

DMT: The full description of the dataset can be accessed in (Timmerman et al. 2021,2023). Twenty-five participants were considered for the experiment in a single-blind, placebo-controlled, and counter-balanced design. To be considered the participants were required to be older than 18 years of age, lack experience with a psychedelic, not have a previous negative response to a psychedelic and/or to currently suffer from or have a history of psychiatric or physical illness. Twenty participants completed the entire study (average age = 33.5 years, SD = 7.9, 7 female). Seventeen participants were used in the analysis after further removal of three participants due to excessive motion during the 8 minutes DMT recording (more than 15% of volumes scrubbed with framewise displacement (FD) of 0.4 mm).

LSD: The full description of the dataset can be accessed in (Carhart-Harris, Muthukumaraswamy, et al., 2016). Twenty healthy participants were considered for the experiment (four females, average age = 30.9 ± 7.8 years) in balanced order, within-participants design. To be considered the participants were required to be older than 21 years of age, not pregnant, to not have personal history of diagnosed psychiatric illness, to not have immediate family history of a psychotic disorder, to not have previous experience with other classical psychedelic drugs, to not have any psychedelic drug use within six weeks of the first scanning day, pregnancy, to not have problematic alcohol use (i.e., >40 units consumed per week), or a medically significant condition. Fifteen subjects were considered for the current analysis. Fifteen participants were used in the analysis after a further removal of one participant due to scanner anxiety and of four participants due to excessive motion during the recording (more than 15% of volumes scrubbed with framewise displacement (FD) of 0.5 mm).

Psilocybin: The full description of the dataset can be accessed in (Carhart-Harris et al., 2012). Fifteen participants were considered for the experiment in a counter-balanced design. To be considered the participants were required to be older than twenty-one years of age, not be pregnant, not to have a history of psychiatric disorders, not to have a cardiovascular disease, not to have a substance dependence, not to have a claustrophobia, not to have a blood or needle phobia, or to have an adverse response to hallucinogens. Furthermore, six participants were excluded if they exceeded 0.4 mm of the mean framewise displacement

Experimental Paradigm

DMT: Every participant underwent two days of scanning, separated by two weeks, with two scanning sessions in each day. The first scan's duration was twenty-eight minutes in an eyes-closed condition (with an eye-mask). The eighth minute marked administration of the intravenous DMT or placebo (saline) (50/50, DMT/Placebo). Subjective effects assessment was carried out after the scanning. For the second session the same protocol was carried but with the assessment of subjective intensity scores. Furthermore, simultaneous EEG was recorded during the sessions.

LSD: Every participant underwent three scanning sessions. The scan duration was carried out after sixty minutes acclimatization period from the bolus injections (over 2 minutes) with LSD (75 μg in 10 ml saline). Three fMRI scans were carried out: rest 1 - eyes-closed resting-state session, rest 2 - resting-state session while listening to music, rest 3 - eyes-closed resting-state session. After each scan Visual Analog Scale (VAS) rating was carried out for each participant. We report results for the average of resting state one and resting state three scans.

Psilocybin: Every participant underwent two days of scanning, separated by minimum of one week. The scan duration lasted twelve minutes with six minutes of recording followed by intravenous administration of either psilocybin (2 mg dissolved in 10 mL of saline, 60-s injection) or a placebo (10 mL of saline, 60-s injection) in an eyes-closed condition. After each scan Visual Analog Scale (VAS) rating was carried out for each participant.

Acquisition Parameters

DMT: A 3T scanner (Siemens Magnetom Verio syngo MR 12 with compatibility for EEG recording) was used for the experiment with T2-weighted echo planar sequence and T1-weighted structural scans. Relevant to the analysis in this paper, the scanning parameters were: TR/TE = 2000ms/30ms, acquisition time = 28.06 minutes, flip angle = 80o, voxel size = 3x3x3 mm3 and 35 slices with 0 mm interslice distance.

LSD: A 3T scanner (GE HDx system) was used for the experiment. High-resolution anatomical images were acquired with 3D fast spoiled gradient echo scans in an axial orientation, with a field of view = 256 × 256 × 192 and matrix = 256 × 256 × 129 to yield 1-mm isotropic voxel resolution. TR/TE = 7.9/3.0 ms; inversion time = 450 ms; flip angle = 20. BOLD-weighted fMRI data were acquired using a gradient-echo planar imaging sequence, TR/TE = 2,000/35 ms, field of view = 220 mm, 64 × 64 acquisition matrix, parallel acceleration factor = 2, 90 flip angles. Thirty-five oblique

axial slices were acquired interleaved, each 3.4 mm thick with zero slice gap (3.4-mm isotropic voxels). The precise length of each of the scans was 7 min 20 s.

Psilocybin: Identical acquisition was carried out for the psilocybin dataset with the following exceptions: fMRI data were acquired at TR/TE = 3,000/35 ms, field of view = 192 mm. Thirty-three oblique axial slices were acquired interleaved, each 3 mm thick with zero slice gap (3 × 3 × 3 mm voxels). The length of the scan was 97 TRs.

fMRI Pre-processing

For fMRI pre-processing, a pipeline developed for Psilocybin (Carhart-Harris et al., 2012) and further applied to LSD (Carhart-Harris et al., 2016) and DMT (Timmermann et al. 2023) experiments was used. Briefly, the following steps were applied 1) despiking, 2) slice-timing correction, 3) motion correction, 4) brain extraction, 5) rigid body registration to structural scans, 6) non-linear registration to 2mm MNI brain, 7) motion-correction scrubbing, 8) spatial-smoothing (FWHM) of 6 mm, 9) bandpass filtering into the frequency range 0.01-0.08 Hz, 10) linear and quadratic detrending, 11) regression of 9 nuisance regressors (3 translations, 3 rotations and 3 anatomical signals). Lastly, the timeseries were parcellated into the Schaefer parcellation of different scales (100, 200, 300, 400, 500 and 1000) in the MNI space.

Temporal asymmetry

We consider two signals $x_i(t)$ and $x_j(t)$. First, we define the (directed) predictive connectivity matrix,

$$D_{ij}(\tau) = \left|CC(x_i(t), x_j(t+\tau))\right| - \left|CC(x_j(t), x_i(t+\tau))\right|$$

where $CC(\cdot,\cdot)$ denotes the Pearson correlation coefficient between the two time series. This expression compares how well the present state of $x_i(t)$ predicts the future state $x_j(t+\tau)$ versus how well the present state of $x_j(t)$ predicts the future state $x_i(t+\tau)$. If $D_{ij}(\tau) > 0$, it suggests that $x_i(t)$ provides more predictive information about $x_j(t+\tau)$ than vice versa, indicating a forward direction of information flow from x_i to x_j. If $D_{ij}(\tau) < 0$, it suggests the opposite direction, and if $D_{ij}(\tau) \approx 0$, no clear directional bias is discerned. By using the symmetry property of circular cross-correlations, we can rewrite $D_{ij}(\tau)$ as

$$D_{ij}(\tau) = \left|CC(x_i(t), x_j(t+\tau))\right| - \left|CC(x_i(t), x_i(t-\tau))\right|.$$

This alternate form shows that $D_{ij}(\tau)$ directly measures how the correlation changes when we shift x_j forward in time by τ seconds versus shifting it backward by τ seconds, relative to $x_i(t)$.

We now define the magnitude of temporal (or thermodynamic) asymmetry matrix as the square value of $D_{ij}(\tau)$.

$$I_{ij}(\tau) = \left(D_{ij}(\tau)\right)^2.$$

If the signals are perfectly time-symmetric, shifting one signal forward or backward by τ seconds yields the same correlation with the other, making $I_{ij}(\tau) = 0$. A nonzero value indicates that the correlation depends on the direction of the time shift, revealing a "break" in temporal symmetry. In other words, $I_{ij}(\tau)$ quantifies how differently the two signals correlate when looking forward versus backward in time, helping to identify processes where the flow of information or causal influence is not symmetric with respect to time.

Finally, we quantify the (scalar) magnitude of this asymmetry using the Fano factor F, which is obtained as the ratio between the mean and standard deviations of all entries in the $I_{ij}(\tau)$:

$$F = \frac{\mu_I}{\sigma_I} \tag{3}$$

Where μ_A and σ_A are the mean and standard deviation of the magnitude of temporal asymmetry matrix entries, respectively.

Functional gradient organisation of temporal asymmetry

Functional gradients of temporal asymmetry of information flow were calculated using the BrainSpace toolbox https://github.com/MICA-MNI/BrainSpace[26] as implemented in MATLAB. The input is the magnitude of temporal asymmetry matrix I_{ij} obtained for each condition in each dataset represented by a NxN matrices, where N is the number of brain regions within the parcellation.

We initialized the algorithm with "*normalized angle*" kernel, "*principal component analysis*" approach and "*Procrustes analysis*" alignment. This resulted in the following steps of the algorithm: First, each row of the temporal asymmetry matrix I_{ij} was thresholded to retain the top 10% of connections, reflecting the strongest magnitudes of temporal asymmetry for each region. Subsequently, the cosine similarity was computed between the connectivity profiles of different regions to construct a similarity matrix, denoted as S. Cosine similarity quantifies the similarity between two vectors by measuring the cosine of the angle between them, effectively capturing the similarity in their connectivity patterns. The cosine similarity between two vectors $\bar{u}$ and $\bar{v}$ is defined as:

$$coisine\ similarity = \cos(\theta) = \frac{\bar{u} \cdot \bar{v}}{\|\bar{u}\|\|\bar{v}\|} = \frac{\sum_{i=1}^{n} u_i \cdot v_i}{\sqrt{\sum_{i=1}^{n} u_i^2} \cdot \sqrt{\sum_{i=1}^{n} v_i^2}}$$

where $\bar{u} \cdot \bar{v}$ denotes the dot product of $\bar{u}$ and $\bar{v}$, and $\|\bar{u}\|$ and $\|\bar{v}\|$ represent their magnitudes. This similarity matrix S is square and symmetric, encoding the similarity between regions in terms of their temporal asymmetry patterns. Given that a symmetric matrix S can be decomposed as $S = U\Sigma U^T$,

where U is an orthogonal matrix of eigenvectors and Σ is a diagonal matrix of eigenvalues, we employed principal component analysis (PCA) for dimensionality reduction. PCA is a linear technique that transforms the data into a low-dimensional space defined by orthogonal components that maximize variance. For each dataset, gradient analysis was performed on the averaged magnitude of the temporal asymmetry matrix. Individual subjects' matrices were then projected onto the principal components using Procrustes alignment, as facilitated by the BrainSpace toolbox[26].

This dimensionality reduction technique aims to uncover a meaningful low-dimensional representation of the high-dimensional original space (in this case, 400 brain regions from the Schaefer 400 parcellation). In this reduced space, the proximity of two points indicates a similar pattern of temporal asymmetry between two regions, whereas greater separation signifies differing patterns. Each gradient represents an axis of covariance in the similarity between regional patterns of temporal asymmetry. Regions with strong loadings on a particular gradient anchor that gradient, while regions with minimal loadings do not exhibit the associated pattern of variation. Notably, for each condition and subject, these anchor points may differ. The greater the disparity between minimum and maximum anchor points, the more pronounced the pattern of temporal asymmetry along the gradients.

To assess these variations, we quantified how the maximum and minimum values along the first two gradients change in the different conditions by measuring the distance between the two extremes for each gradient named "gradient 1 and 2 surface". Lastly, we quantified the "gradients reshaping" as the mean Euclidean distance traversed by individual regions in the 2-dimensional embedding of the first two gradients between the pre- and post-intervention conditions.

Author Contributions

J.V., Y.S-P., G.D. and M.L.K. conceived the analysis. R.L.C-H designed the original study. J.V., Y.S-P., G.D. and M.L.K. designed and developed the methodologies. J.V. analysed the data. C.T. and L.R. acquired and provided the data. J.V., Y.S-P., R.L.C-H, E.T., E.L-S., E.G-G., G.R. revised the paper and provided critical feedback.

Funding

Jakub Vohryzek is supported by EU H2020 FET Proactive project Neurotwin grant Agreement No. 101017716. Yonatan Sanz-Perl is supported by "ERDF A way of making Europe," ERDF, EU, Project NEurological MEchanismS of Injury, and Sleep-like cellular dynamics (NEMESIS; ref. 101071900) funded by the EU ERC Synergy Horizon Europe. Morten L. Kringelbach is supported by the European Research Council Consolidator Grant: CAREGIVING (615539), Pettit Foundation, Carlsberg Foundation, and Center for Music in the 910 Brain, funded by the Danish National

Research Foundation (DNRF117). Gustavo 911 Deco is supported by the Spanish Research Project PSI2016-75688-P (Agencia 912 Estatal de Investigación/Fondo Europeo de Desarrollo Regional, European Union); 913 by the European Union's Horizon 2020 Research and Innovation Programme 914 under Grant Agreements 720270 (Human Brain Project [HBP] SGA1) and 785907 915 (HBP SGA2); and by the Catalan Agency for Management of University and 916 Research Grants Programme 2017 SGR 1545. Giulio Ruffini and Edmundo Lopez-Sola are partially funded by the European Commission under European Union's Horizon 2020 research and innovation programme Grant Number 101017716 (Neurotwin) and European Research Council (ERC Synergy Galvani) under the European Union's Horizon 2020 research and innovation program Grant Number (855109).

Conflict of Interest

G.R., E.L-S. work for Neuroelectrics, a company developing brain stimulation solutions. R.L.C-H. is an advisor to Otsuka, MindState, and Entheos Labs.

References

1 Siegel, J. S. *et al.* Psilocybin desynchronizes the human brain. *Nature* **632**, 131-138 (2024).
2 Anderson, B. T., Danforth, A. L. & Grob, C. S. Psychedelic medicine: safety and ethical concerns. *The Lancet Psychiatry* **7**, 829-830 (2020).
3 Daws, R. E. *et al.* Increased global integration in the brain after psilocybin therapy for depression. *Nature medicine* **28**, 844-851 (2022).
4 Carhart-Harris, R. L. *et al.* Psilocybin for treatment-resistant depression: fMRI-measured brain mechanisms. *Scientific reports* **7**, 1-11 (2017).
5 Girn, M. *et al.* Serotonergic psychedelic drugs LSD and psilocybin reduce the hierarchical differentiation of unimodal and transmodal cortex. *NeuroImage* **256**, 119220 (2022).
6 Singleton, S. P. *et al.* LSD flattens the brain's energy landscape: evidence from receptor-informed network control theory. *BioRxiv*, in review (2021).
7 Tagliazucchi, E. *et al.* Increased global functional connectivity correlates with LSD-induced ego dissolution. *Curr. Biol.* **26**, 1043-1050 (2016).
8 Vohryzek, J. *et al.* The flattening of spacetime hierarchy of the DMT brain state is characterised by harmonic decomposition of spacetime (HADES) framework. *National Science Review* **11** (2024).
9 Timmermann, C. *et al.* Human brain effects of DMT assessed via EEG-fMRI. *Proceedings of the National Academy of Sciences* **120**, e2218949120 (2023).
10 Carhart-Harris, R. L. & Friston, K. J. REBUS and the anarchic brain: toward a unified model of the brain action of psychedelics. *Pharmacological reviews* **71**, 316-344 (2019).
11 Hilgetag, C. C. & Goulas, A. 'Hierarchy'in the organization of brain networks. *Philosophical Transactions of the Royal Society B* **375**, 20190319 (2020).
12 Kringelbach, M. L., Perl, Y. S. & Deco, G. The Thermodynamics of Mind. *Trends in Cognitive Sciences* (2024).
13 Deco, G., Sanz Perl, Y., Tagliazucchi, E. & Kringelbach, M. L. The INSIDEOUT framework provides precise signatures of the balance of intrinsic and extrinsic dynamics in brain states. *Commun. Biol.* **5**, 572 (2022).
14 Sanz Perl, Y. *et al.* Non-equilibrium brain dynamics as a signature of consciousness. *Physical Review E* **104**, 014411 (2021).

15 Lynn, C. W., Cornblath, E. J., Papadopoulos, L., Bertolero, M. A. & Bassett, D. S. Broken detailed balance and entropy production in the human brain. *Proceedings of the National Academy of Sciences* **118**, e2109889118 (2021).
16 Deco, G. *et al.* Different hierarchical reconfigurations in the brain by psilocybin and escitalopram for depression. *Nature Mental Health* **2**, 1096-1110 (2024).
17 Pasquini, L. *et al.* Long-term effects of psilocybin on dynamic and effectivity connectivity of fronto-striatal-thalamic circuits. *bioRxiv*, 2024.2011. 2006.622302 (2024).
18 Deco, G. *et al.* The arrow of time of brain signals in cognition: Potential intriguing role of parts of the default mode network. *Network Neuroscience* **7**, 966-998 (2023).
19 Kringelbach, M. L., Perl, Y. S., Tagliazucchi, E. & Deco, G. Toward naturalistic neuroscience: Mechanisms underlying the flattening of brain hierarchy in movie-watching compared to rest and task. *Science Advances* **9**, eade6049 (2023).
20 G.Guzman, E. *et al.* The lack of temporal brain dynamics asymmetry as a signature of impaired consciousness states. *Interface Focus* **13**, 20220086 (2023). https://doi.org/10.1098/rsfs.2022.0086
21 Carhart-Harris, R. L. *et al.* Neural correlates of the psychedelic state as determined by fMRI studies with psilocybin. *Proceedings of the National Academy of Sciences* **109**, 2138-2143 (2012).
22 Carhart-Harris, R. L. *et al.* Neural correlates of the LSD experience revealed by multimodal neuroimaging. *Proceedings of the National Academy of Sciences* **113**, 4853-4858 (2016).
23 Schaefer, A. *et al.* Local-global parcellation of the human cerebral cortex from intrinsic functional connectivity MRI. *Cereb. Cortex* **28**, 3095-3114 (2018).
24 Gnesotto, F. S., Mura, F., Gladrow, J. & Broedersz, C. P. Broken detailed balance and non-equilibrium dynamics in living systems: a review. *Reports on Progress in Physics* **81**, 066601 (2018).
25 Yeo, B. T. T. *et al.* The organization of the human cerebral cortex estimated by intrinsic functional connectivity. *J Neurophysiol* (2011).
26 Vos de Wael, R. *et al.* BrainSpace: a toolbox for the analysis of macroscale gradients in neuroimaging and connectomics datasets. *Communications biology* **3**, 103 (2020).
27 Margulies, D. S. *et al.* Situating the default-mode network along a principal gradient of macroscale cortical organization. *Proceedings of the National Academy of Sciences* **113**, 12574-12579 (2016).
28 Esposito, U., Giugliano, M., Van Rossum, M. & Vasilaki, E. Measuring symmetry, asymmetry and randomness in neural network connectivity. *PloS one* **9**, e100805 (2014).
29 Li, Z. & Dayan, P. Computational differences between asymmetrical and symmetrical networks. *Advances in Neural Information Processing Systems* **11** (1998).
30 Siegelmann, H. T. & Sontag, E. D. in *Proceedings of the fifth annual workshop on Computational learning theory*. 440-449.
31 Lukoševičius, M. & Jaeger, H. Reservoir Computing Approaches to Recurrent Neural Network Training. *Computer Science Review* **3**, 127-149 (2009).
32 Rajan, K., Abbott, L. & Sompolinsky, H. Stimulus-dependent suppression of chaos in recurrent neural networks. *Physical Review E—Statistical, Nonlinear, and Soft Matter Physics* **82**, 011903 (2010).
33 Lord, L. D. *et al.* Dynamical exploration of the repertoire of brain networks at rest is modulated by psilocybin. *NeuroImage* **199**, 127-142 (2019).
34 Atasoy, S., Deco, G. & Kringelbach, M. L. in *The Functional Role of Critical Dynamics in Neural Systems* (eds M. Herrmann, N. Tümen, & U. Ernst) 27-45 (Springer, 2019).
35 Atasoy, S., Deco, G., Kringelbach, M. L. & Pearson, J. Harmonic brain modes: a unifying framework for linking space and time in brain dynamics. *The Neuroscientist* **24**, 277-293 (2018).
36 Ruffini, G., Lopez-Sola, E., Vohryzek, J. & Sanchez-Todo, R. Neural geometrodynamics, complexity, and plasticity: a psychedelics perspective. *Entropy* **26**, 90 (2024).

37 Juliani, A., Safron, A. & Kanai, R. Deep CANALs: a deep learning approach to refining the canalization theory of psychopathology. *Neuroscience of Consciousness* **2024**, niae005 (2024).
38 Langton, C. G. Computation at the edge of chaos: Phase transitions and emergent computation. *Physica D: nonlinear phenomena* **42**, 12-37 (1990).
39 England, J. L. Dissipative adaptation in driven self-assembly. *Nature nanotechnology* **10**, 919-923 (2015).
40 England, J. L. Statistical physics of self-replication. *The Journal of chemical physics* **139** (2013).
41 Landauer, R. Irreversibility and heat generation in the computing process. *IBM journal of research and development* **5**, 183-191 (1961).
42 Karl, F. A free energy principle for biological systems. *Entropy* **14**, 2100-2121 (2012).
43 Fang, X., Kruse, K., Lu, T. & Wang, J. Nonequilibrium physics in biology. *Reviews of Modern Physics* **91**, 045004 (2019).
44 Battle, C. *et al.* Broken detailed balance at mesoscopic scales in active biological systems. *Science* **352**, 604-607 (2016).
45 Esposito, M. Stochastic thermodynamics under coarse graining. *Physical Review E* **85**, 041125 (2012).
46 Kringelbach, M. L., Sanz Perl, Y., Tagliazucchi, E. & Deco, G. Toward naturalistic neuroscience: Mechanisms underlying the flattening of brain hierarchy in movie-watching compared to rest and task. *Science advances* **9**, eade6049 (2023).
47 de la Fuente, L. *et al.* Temporal irreversibility of neural dynamics as a signature of consciousness. *Cereb. Cortex*, bhac177 (2022). https://doi.org/10.1101/2021.09.02.458802
48 Ruffini, G. An algorithmic information theory of consciousness. *Neuroscience of Consciousness* **2017**, nix019 (2017).
49 Ruffini, G., Castaldo, F., Lopez-Sola, E., Sanchez-Todo, R. & Vohryzek, J. The algorithmic agent perspective and computational neuropsychiatry: from etiology to advanced therapy in major depressive disorder. *Entropy* **26**, 953 (2024).
50 Ruffini, G. & Lopez-Sola, E. AIT foundations of structured experience. *Journal of Artificial Intelligence and Consciousness* **9**, 153-191 (2022).
51 Prigogine, I. & Nicolis, G. On symmetry-breaking instabilities in dissipative systems. *The Journal of Chemical Physics* **46**, 3542-3550 (1967).
52 Bennett, C. H. The thermodynamics of computation—a review. *International Journal of Theoretical Physics* **21**, 905-940 (1982).
53 Ohga, N., Ito, S. & Kolchinsky, A. Thermodynamic bound on the asymmetry of cross-correlations. *Physical Review Letters* **131**, 077101 (2023).
54 Bressler, S. L. & Seth, A. K. Wiener–Granger causality: a well established methodology. *Neuroimage* **58**, 323-329 (2011).
55 Seth, A. K., Barrett, A. B. & Barnett, L. Granger causality analysis in neuroscience and neuroimaging. *Journal of Neuroscience* **35**, 3293-3297 (2015).
56 Deco, G., Lynn, C. W., Sanz Perl, Y. & Kringelbach, M. L. Violations of the fluctuation-dissipation theorem reveal distinct non-equilibrium dynamics of brain states. *Physical Review E*, in press (2023).